Electronic Supplementary Material (ESI) for Physical Chemistry Chemical Physics.

Supporting Information for

Optimizing photon upconversion by decoupling excimer formation and triplet triplet annihilation

Chen Ye,[a] Victor Gray,[b,c] Khushbu Kushwaha,[a] Sandeep Kumar Singh,[d] Paul Erhart,[d] and Karl Börjesson[a]*

AUTHOR ADDRESS

a Dr. C. Ye, Dr. K. Kushwaha, Dr. K. Börjesson
Department of Chemistry and Molecular Biology, University of Gothenburg, 41296 Gothenburg, Sweden.
E-mail: karl.borjesson@gu.se

b Dr. V. Gray
Department of Chemistry–Ångström Laboratory, Uppsala University, 75120, Uppsala, Sweden.

c Dr. V. Gray
Department of Physics, Cavendish Laboratory, University of Cambridge, 19 JJ Thompson Avenue, Cambridge, CB3 0HE, UK.

d Dr. S. K. Singh, Prof. Dr. P. Erhart
Department of Physics, Chalmers University of Technology, 41296 Gothenburg, Sweden.

1. Experimental Section

1.1 TTA-UC sample preparation

All TTA-UC samples were prepared in an Mbraun glove box having oxygen and water levels less than 1 ppm. Cuvettes were sealed with cap and PTFE septum. Photon upconversion measurements were performed immediately after the preparation.

1.2 Steady state emission

Steady state emission of TTA-UC samples with PtTBTP was measured on an Edinburgh Instruments FLS 1000 spectrofluorometer. A Light Emitting Diode (LED) with collimator and focus lenses was used as a non-coherent excitation source. Emission was collected 90 degrees as compared to the excited light. The LED light source (617 nm, Thorlabs M617L3 mounted LED), power supply and all the optical units were purchased from Thorlabs, Inc. The connection and supporting units were home-made from non-fluorescent plastic[2] by 3D-printing.

1.3 Quantum yield calculations.

The photoluminescence quantum yield of the luminescent species were determined from an indirect method with standard reference as recommend by IUPAC.[3] The quantum yield of the testing samples (Φ_S) were calculated by the following equation:

$$\Phi_S = \Phi_R \times \frac{\int F_S(\lambda)\, d\lambda}{\int F_R(\lambda)\, d\lambda} \times \left(\frac{n_S}{n_R}\right)^2 \times \frac{I_R}{I_S} \times \frac{1 - 10^{-A_R}}{1 - 10^{-A_S}} \quad (eq.S1)$$

where Φ_R is the fluorescence quantum yield of the reference sample, $F_i(\lambda)$ is the emission intensity function, n_i is the refractive index of the solvent, I_i is the excitation intensity, and A_i is the absorbance of the sample at the excitation wavelength. Standard reference materials were selected by the excitation and emission spectrum range according to

IUPAC recommendations. Quinine sulphate in H_2SO_4 solution was used as reference for calculating the fluorescence quantum yields of perylene derivatives (Φ_R = 0.52). Cresyl violet was used as reference for calculating the photon upconversion quantum yields (Φ_R = 0.57). For TTA-UC with perylene as the annihilator, the emission of monomer is integrated from 400 to 540 nm, due to the low intensity of perylene monomer emission outside this range. The excimer emission is integrated from 540 nm to 700 nm.

1.4 Time resolved spectroscopy

Phosphorescence quenching was measured on an Edinburgh FLS 1000 spectrofluorometer with a microsecond flash lamp as excitation source. Prompt fluorescence decay was recorded by time-correlated single photon counting (TCSPC) on Edinburgh FLS 1000 spectrofluorometer with a pulsed diode laser (375 nm, 1 MHz) as the excitation source and MCP-PMT as detector. Phosphorescence and delayed fluorescence decays were recorded by time-correlated single photon counting on Edinburgh FLS 1000 spectrofluorometer with a pulsed diode laser (375 nm, 1 MHz) as the excitation source and MCP-PMT as the detector. Fluorescence decay was recorded by multi-channel scaling (MCS) on Edinburgh FLS 1000 spectrofluorometer with a pulsed microsecond flash lamp (617 nm, 100 Hz) as the excitation source and PMT-900 as the detector.

Transient absorption was measured on an Edinburgh Instrument LP 980 spectrometer, with a Spectra-Physics Nd:YAG laser (617 nm, pulse width ~7 ns) coupled to a Spectra-Physics primoscan optical parametric oscillator (OPO) as excitation. PMT (Hamamatsu R928) or image intesified CCD camera (ICCD, Andor DH320T-25F-03) detectors were used for recording transient kinetics or spectra, respectively.

1.5 Rate determination step of TET

TET from the sensitizer involves diffusion and energy transfer. The diffusion constant k_{diff} is estimated by the following equation:

$$k_{diff} = \frac{8RT}{3\eta} \quad (eq.S2)$$

where *R* is the ideal gas constant, *T* is the absolute temperate, η is the viscosity of the solvent. The k_{diff} is 1.4×10^{10} $M^{-1}s^{-1}$ at room temperature in THF. The calculated k_{TET} is smaller than k_{diff}, and thus the quenching is TET limited.

1.6 Density functional theory (DFT) calculations.

The effect of excitations on the interaction between a pair of perylene molecules was analysed within the framework of time-dependent density functional theory (TDDFT). Calculations were carried out using the B3LYP functional[4] with dispersion corrections (D3BJ)[5] and the 6−311G* basis set[6] as implemented in the NWChem suite[7]. This approach closely follows our earlier calculations[1].

1.7 The effective and average TTA reaction radii of perylene and perylene derivatives.

Diffusion coefficients (*D*) in solutions can be calculated by the empirical correlation developed by Wilke Chang.[8]

$$D = 7.4 \times 10^{-8} \frac{(xM)^{0.5}T}{\eta V^{0.6}} \quad (eq.S3)$$

where *x* is the association number of solvent, M is the molecular weight of solute, T is the temperature, η is the viscosity of the solvent, and V is the molecular volume of the solvent.

Based on the analysis of time resolved spectroscopy, we got the apparent kinetic parameters (k_{TTA}, k_T, R_{TTA}) for TTA with the different annihilators. To compare the four annihilators, we want to calculate the mean TTA interaction distance (d_{TTA}). The TTA time window relies on the lifetime, which greatly exceeds the diffusion time character ($\tau >> R_{TTA}^2/D$). We can treat the distribution of triplet excited annihilator through diffusion as a fast process before TTA. Triplet-triplet annihilation is a typical case of a bi-molecular photophyscial transformation, which involves the diffusion of excited species. In our work, we show the difference of four annihilator molecules on TTA-UC and discuss the advantages and disadvantages of alkylation of perylene on TTA-UC. To make the mechanism more clear and intuitive, we want to take the relative motion of two triplet excited species into account in the analysis. We treat the first triplet excited annihilator as stationary, as a nearby second triplet excited annihilator approaches. The relative motion of the mobile component to the static component follows Fick's second law of diffusion with an interaction term (eq. S4):

$$\frac{\partial \rho}{\partial t} = D\nabla^2\rho - k_T\rho - 2k_{TTA}\rho^2 \quad (eq.S4)$$

where $\rho = C/C_0$ is the time and spatial dependent density (normalized concentration) of the triplet excited annihilator, and $\nabla = \partial/\partial \mathrm{r}$ is the Laplace operator in radial coordinates. When approximating steady state conditions, we assume a spatially independent density ($D\nabla^2\rho = 0$), which reduces eq. S4 to an ordinary differential equation (eq. 3; Figure 3c). To take the spatial distribution of molecules into account in eq S2, we assume that TTA is a diffusion limited process (eq. S5):

$$\frac{\partial \rho}{\partial t} = D\frac{\partial^2 \rho}{\partial r^2} \quad (eq.S5)$$

The annihilator interaction range ($r = R_{TTA}$) is the intermolecular distance for complete TTA reaction (100% efficient trapping). At the initial time, the reacting molecules are randomly distributed with a uniform concentration outside the complete reaction zone. Given that TET is fast and efficient, the boundary conditions of a statistical distribution outside the annihilator interaction range can be described as below:

$$\rho_{(r,t=0)} = 0 \text{ for } r \leq R_{TTA}$$

$$\rho_{(r,t=0)} = 1 \text{ for } r > R_{TTA}$$

Marian Smoluchowski found the solution of eq. S3 with the above Dirichlet boundary conditions,[9]

$$\rho(r,t) = 1 - \frac{R_{TTA}}{r}\,\mathrm{erfc}\left[\frac{r - R_{TTA}}{2\sqrt{DT}}\right] \quad (eq.S6)$$

$$\rho(r,\infty) = 1 - \frac{R_{TTA}}{r} \quad (eq.S7)$$

where erfc(x) is the complementary error function. With increasing time, the distribution function turns to a steady-state expression (eq. S7). As shown in figure below, the distribution of triplet excited annihilators reach stationary conditions at the beginning of the TTA process, indicating that our approximation is reasonable.

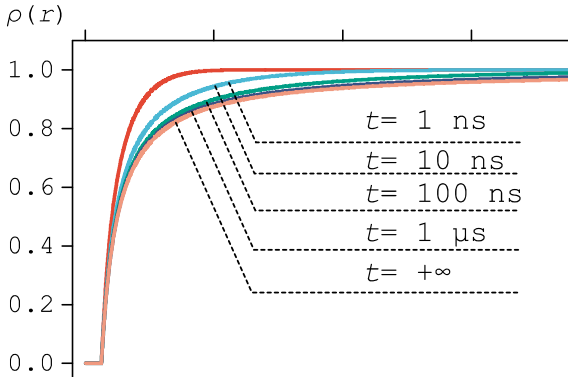

Normalized theoretical density of triplet excited annihilator as a function of intermolecular distance at different times after triplet formation.

The reaction rate of TTA is based on the flux of molecules at the encounter distance. The apparent rate constant of TTA then satisfies the following expression (eq. S8):

$$k_{TTA} = 4\pi N R_{TTA}^2 D \frac{\partial \rho(r)}{\partial r} = 4\pi D N R_{TTA}\left[1 + \frac{R_{TTA}}{(\pi D t)^{1/2}}\right] \quad (eq.S8)$$

where at the TTA time scale, t is much larger than the diffusion characteristic time R_{TTA}^2/D, and the rate equation converts to the steady-state expression (eq. 5; Table 1). TTA is a special case of Dexter energy transfer, in which excited electrons are transferred between two annihilator molecules via a non-radiative path. The Dexter energy transfer process requires enough overlap between the two electron clouds, and it is thus only effective within a very short range (~10 Å).[10] The annihilation rate constant therefore follow the Dexter energy transfer formulation (eq. S9):[11]

$$k_{Dex}(r) = k_0 exp\left(\frac{-2r}{L}\right) \quad (eq.S9)$$

where *L* is average Bohr radius of the chromophores. The Dexter energy transfer rate decreases dramatically when increasing the donor-acceptor distance. Based on this, we can calculate the spatially dependent TTA reaction possibility by the following formula (eq. S10):

$$\rho_r(r) = \frac{k_{Dex}(r)}{k_0}\rho(r) \quad (eq.S10)$$

The steady-state distribution and TTA reaction probability is shown below. By integrating the reaction probability in radial coordinates, we calculated the mean TTA interaction distance of **pery**, **et-pery**, ***t*-bu-pery** and **t-*t*-bu-pery** to be 1.44 nm, 1.26 nm, 1.31 nm, and 1.03 nm, respectively (eq. S11). From these numbers it is clear that large steric groups reduce the active zone for TTA interaction, and is thus unfavourable for building efficient TTA-UC systems. The trend for the mean TTA interaction (d_{TTA}) also follows the effective interaction (R_{TTA}, Table 1).

$$d_{TTA} = \frac{\int_{R_{TTA}}^{\infty} 4\pi r^2\, \rho_r(r)\, r\, dr}{\int_{R_{TTA}}^{\infty} 4\pi r^2\, \rho_r(r)\, dr} \quad (eq.S11)$$

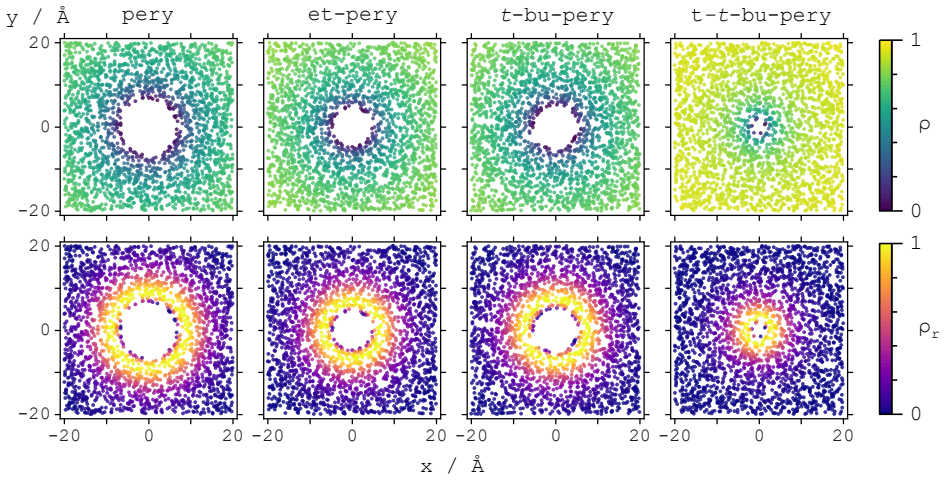

Normalized theoretical density of triplet excited annihilator around a fixed annihilator and the corresponding normalized TTA reaction probability by Monte Carlo simulations under steady-state approximations.

2. Figures cited in the main text.

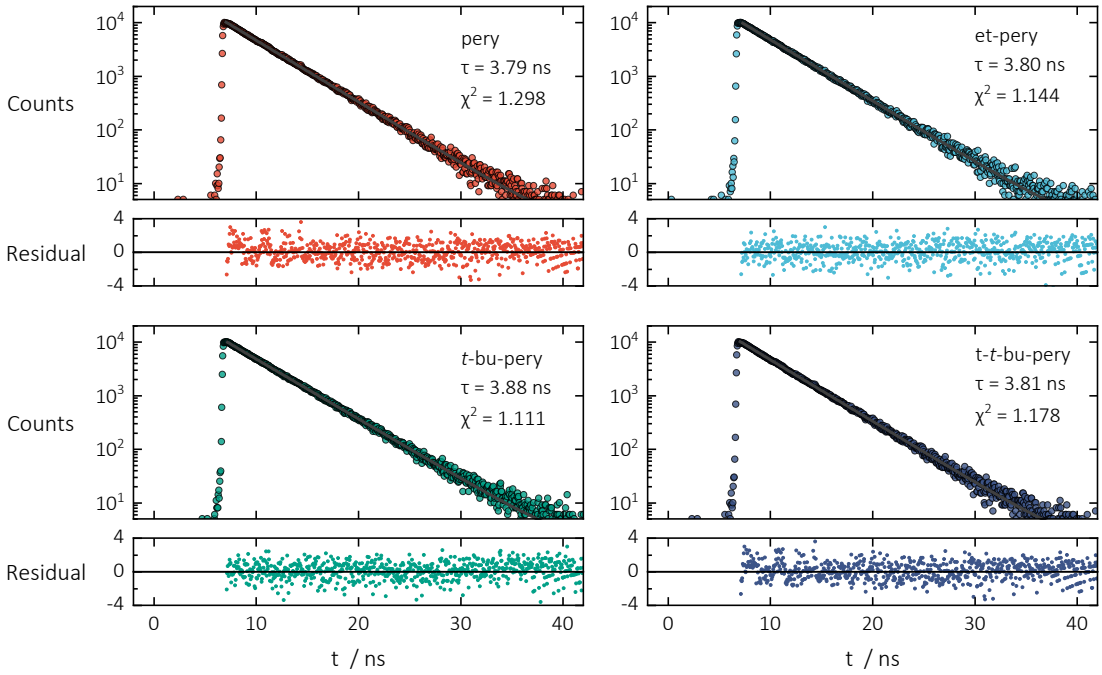

Figure S1. Time resolved photoluminescence decay of perylene and perylene derivatives (10 μM) in THF. The excitation and detection wavelengths are 375 nm and 445 nm, respectively.

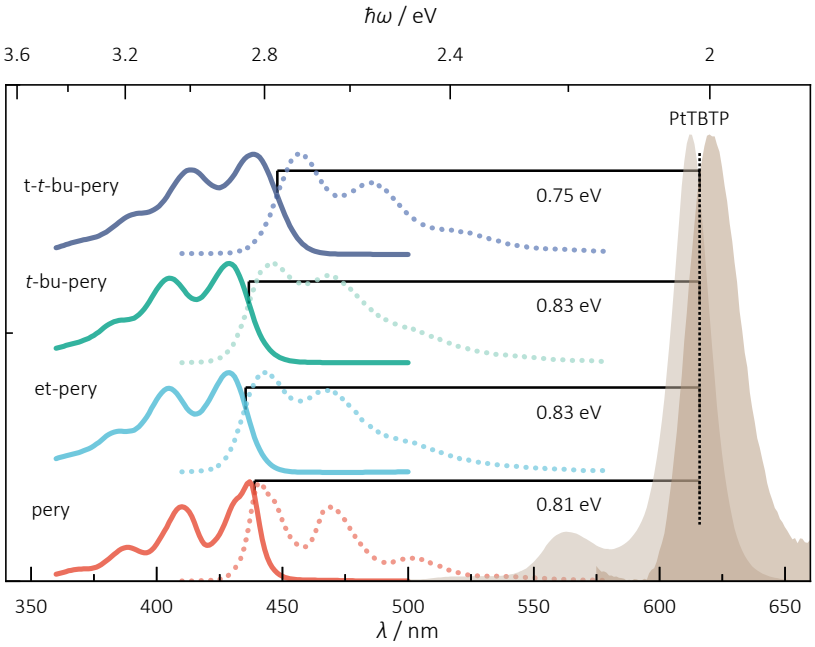

Figure S2. Absorption and emission spectrum of **PtTBTP**, **pery**, **et-pery**, ***t*-bu-pery** and **t-*t*-bu-pery** in THF. Stokes shifts are labelled as the differences of E_{00} values from annihilators to sensitizer. Note that the porphyrin emission is the weak fluorescence signal from this molecule.

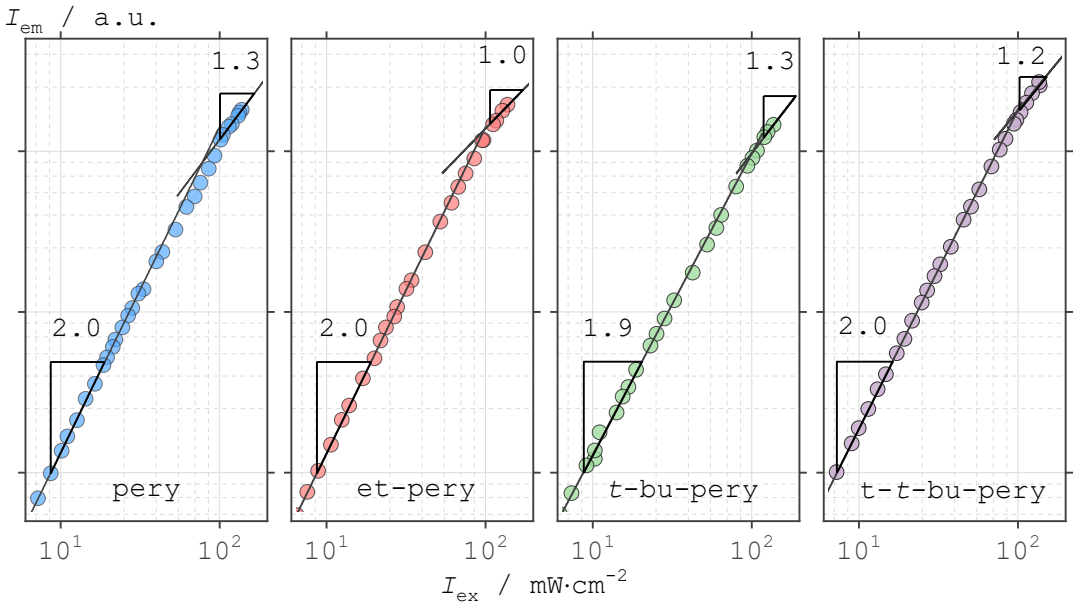

Figure S3. Upconversion intensity of 10 μM sensitizer and 1 mM annihilator in THF at different excitation power

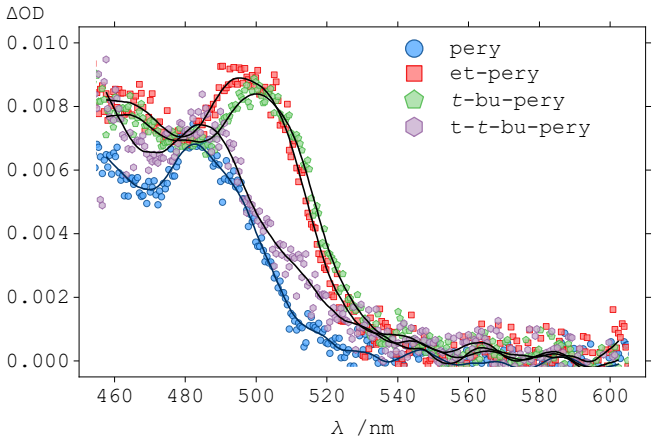

Figure S4. Transient absorption spectrum of 1mM **pery**, **et-pery**, ***t*-bu-pery** and **t-*t*-bu-pery** in THF with 10 µM PtTBTP as sensitizer. All these samples are excited at 617 nm.

3. References

[1] K. Kushwaha, L. Yu, K. Stranius, S. K. Singh, S. Hultmark, M. N. Iqbal, L. Eriksson, E. Johnston, P. Erhart, C. Muller, K. Börjesson, *Adv. Sci.* **2019**, *6*, 1801650.

[2] B. Joarder, N. Yanai, N. Kimizuka, *J. Phys. Chem. Lett.* **2018**, *9*, 4613-4624.

[3] A. M. Brouwer, *Pure Appl. Chem.* **2011**, *83*, 2213-2228.

[4] a) C. Lee, W. Yang, R. G. Parr, *Phys. Rev. B* **1988**, *37*, 785-789; b) A. D. Becke, *J. Chem. Phys.* **1993**, *98*, 5648-5652.

[5] S. Grimme, J. Antony, S. Ehrlich, H. Krieg, *J. Chem. Phys.* **2010**, *132*, 154104.

[6] a) A. D. McLean, G. S. Chandler, *J. Chem. Phys.* **1980**, *72*, 5639-5648; b) R. Krishnan, J. S. Binkley, R. Seeger, J. A. Pople, *J. Chem. Phys.* **1980**, *72*, 650-654.

[7] M. Valiev, E. J. Bylaska, N. Govind, K. Kowalski, T. P. Straatsma, H. J. J. Van Dam, D. Wang, J. Nieplocha, E. Apra, T. L. Windus, W. A. de Jong, *Comput. Phys. Commun.* **2010**, *181*, 1477-1489.

[8] C. R. Wilke, P. Chang, *AIChE J.* **1955**, *1*, 264-270.

[9] M. v. Smoluchowski, *Z. Phys. Chem.* **1918**, *92*, 129.

[10] T. Mirkovic, E. E. Ostroumov, J. M. Anna, R. van Grondelle, Govindjee, G. D. Scholes, *Chem. Rev.* **2017**, *117*, 249-293.

[11] S. Faure, C. Stern, R. Guilard, P. D. Harvey, *J. Am. Chem. Soc.* **2004**, *126*, 1253-1261.